# Automatic atlas-based segmentation of the prostate: A MICCAI 2009 Prostate Segmentation Challenge entry

Jason Dowling[1], Jurgen Fripp[1], Peter Greer[2,3], Sébastien Ourselin[4] , Olivier Salvado[1],

[1] Australian e-Health Research Centre, CSIRO ICT Centre, Australia
jason.dowling@csiro.au
[2] Calvary Mater Newcastle Hospital, Australia
[3] University of Newcastle, Australia Peter.Greer@mater.health.nsw.gov.au
[4] Centre for Medical Image Computing, University College London, UK

**Abstract.** This paper presents a method for the automatic segmentation of the prostate from pelvic axial magnetic resonance (MR) images incorporating non-rigid registration with probabilistic atlases (PAs) as part of the 2009 MICCAI prostate segmentation challenge. This scheme was trained and evaluated on two sets of small field of view prostate images comprising (i) a set of 15 T2w Fast Spin Echo (FSE) axial MR images; and (ii) a single axial FSE axial MR image; both acquired with surface coils. Our scheme involves several steps, including (i) generation of PAs for the prostate and (ii) segmentation using non-rigid registration based propagation of the PAs. A population of preprocessed images were used to build an average shape atlas. The PAs for the prostate were generated for this atlas by propagating each subject's manual segmentations. Segmentation was performed by registering the atlas to each preprocessed image and propagating and thresholding the PAs. The automatic segmentation results were compared to the manual segmentations using the Dice Similarity Coefficient (DSC) with a median DSC for the prostate of 0.76.

## 1 Introduction

The 2009 MICCAI prostate segmentation challenge was held as a workshop of MICCAI 2009 in London, UK with the aim of discussing the state-of-art segmentation of Prostate MRI in the context of MRI-guided prostate therapy, through comparison of the segmentation methods using sample data.

There are few papers on prostate segmentation from MRI (most have focused on ultrasound and CT), however recent papers by Martin et al. [1] and Klein et al. [2]

have proposed the use of an automatic prostate segmentation method based on non-rigid registration of a set of pre-labeled MR atlas images. Atlas based segmentation usually involves an atlas image (generally an average of a set of images) with a matching set of organ labels. To segment a new image, the atlas is registered to the the subjects' image to obtain a good correspondence between structurally equivalent regions in the two images, and then labels defined on the atlas are propagated to the image [3]. In this paper an atlas-based approach is applied which involves the automatic segmentation of the prostate from pelvic axial MR images by generating an average image atlas incorporating non-rigid registration with probabilistic atlases (PAs). The work presented in this paper is similar to Klein et al. [2]: the main difference is that instead of identifying a selection of atlas scans which are most similar to the target scan and using only their associated deformed label images, in this paper a single prostate atlas is used.

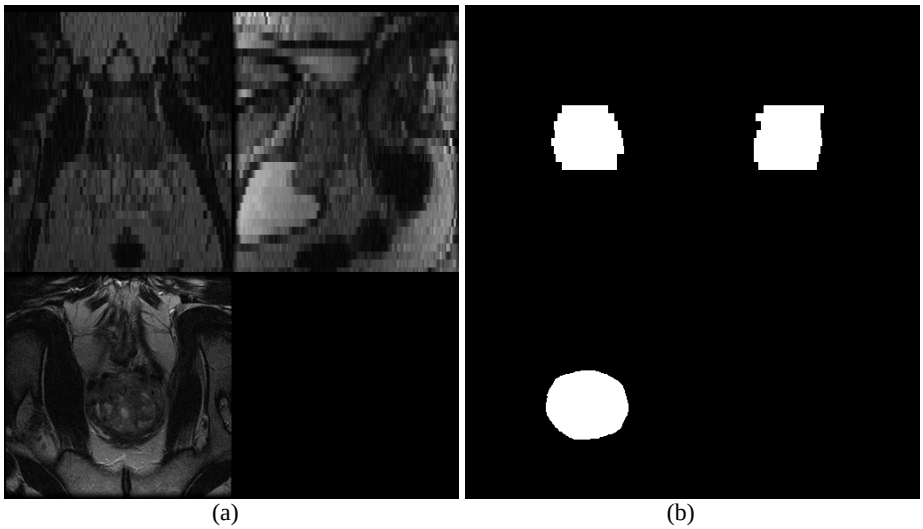

(a) (b)

**Fig. 1.** Coronal, Sagittal and Axial views of training volume 28 (with manual prostate segmentation on the right), which was used as the initial atlas case for atlas generation.

## 2 Method

### 2.1 MR Images

The training set comprised 15 anonymized patient datasets. These consisted of Fast Spin Echo (FSE) T1w and T2w axial MR images. All images were taken in a 1.5T scanner. Expert segmentation of the prostate from the T2w scans were also provided. In addition a single test image was provided for evaluation (also T2w FSE MRI).

These images were downloaded in nrrd format from the challenge url: http://prostatemrimagedatabase.com . The T1w images were not used in this work.

### 2.2 Atlas Generation

A probabilistic atlas (PA) for the prostate was generated by propagating the manual segmentations of for each training case using the obtained affine transform and deformation field computed from the MR into the atlas space as per Rohlfing [4] . An arbitrary but representative case in our database was chosen as the initial atlas (case 28 shown in Figure 1), defining the atlas space alignment

.

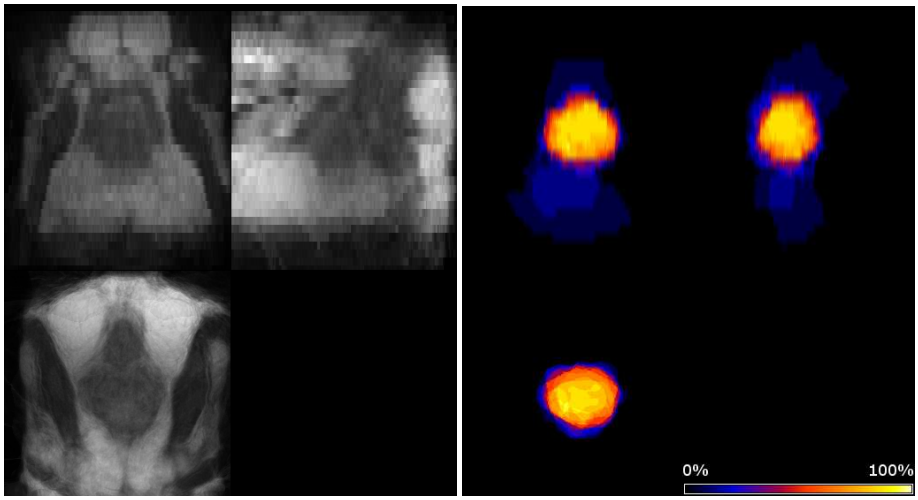


(a) (b)

**Fig. 2**. (a) Coronal, Sagittal and Axial views of the generated average shape atlas, with (b) showing the associated probabilistic maps of the prostate (lighter intensity = higher agreement between segmentations).

The first iteration involved the registration of every other case to the selected atlas case using rigid and affine transformation. Subsequent iterations involved all subjects being registered to the average image using rigid, affine and non-rigid registration. At the end of each iteration a new average atlas is generated and used in the subsequent iteration. In the present study, three iterations were performed. We used the Insight Toolkit (www.itk.org) implementation of the free-form deformation algorithm [5] for non-rigid registration. After rigid and affine initialization of the transformation, a displacement field modeled as a linear combination of B-splines is estimated by the maximization of the Mattes mutual information [6] between the two volumes. A regular grid of uniformly distributed control points and a gradient descent optimizer were used. A four level coarse-to-fine pyramidal based approach was used where each pyramidal level doubled the image resolution and the number of control points.

### 2.2 Automatic Segmentation

After generation of the probabilistic atlas it is used to identify the prostate. from surrounding tissue on a new subject in the following way. Rigid, affine and non-rigid registration were used to map the atlas onto each subject's MR scan and the affine transform and deformation fields were then used to map the prostate PA onto each scan. The prostate PA was then thresholded to provide a general segmentation for each individual subject. The automatic segmentations were compared against manual segmentations using the Dice Similarity Coefficient (DSC = 2 ( A ∩ B / (A union B) )) [7].

## 3. Results

Using affine registration followed by the non-rigid registration, the automatic segmentation for each MR scan required approximately 60 minutes on a standard desktop PC ( Intel Dual Core @ 3 GHz, 2Gb RAM).

The generated average shape atlas is presented in Figure 2(a) with the associated probabilistic segmentations of the prostate should in 2(b).

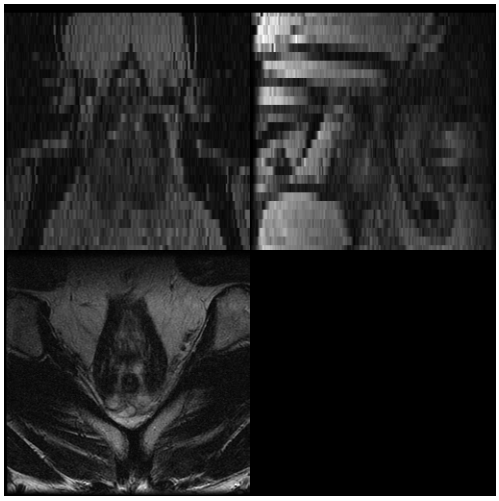

**Fig. 3**. Coronal, Sagittal and Axial views of the test volume (PatientID = 132).

An example of applying the average shape atlas to automatically segment the test scan is shown in Figures 3 to 5. Coronal, Sagittal and Axial views of the original test MRI are shown in Figure 3. Figure 4(a) displays the result of affine and non-rigid registration of the average shape atlas to this subject. The expert manual segmentation for this volume were not made available (for blind assessment by the

workshop organizers), however Figure 5 presents a qualitative demonstration of segmentation accuracy with (a) the segmentation boundary overlaid on a single axial slice, and (b) a surface mesh generated from the automatic prostate segmentation overlaid on a 3D view of the patient scan.

The DSC results for all cases are summarized in Figure 6. Unfortunately the registration failed for three of the cases due to significant bias field artefacts in these scans (future work will investigate the correction of these artefacts). The mean DSC Overlap for the remaining cases was 0.73 (sd = 0.11), with a median DSC of 0.78.

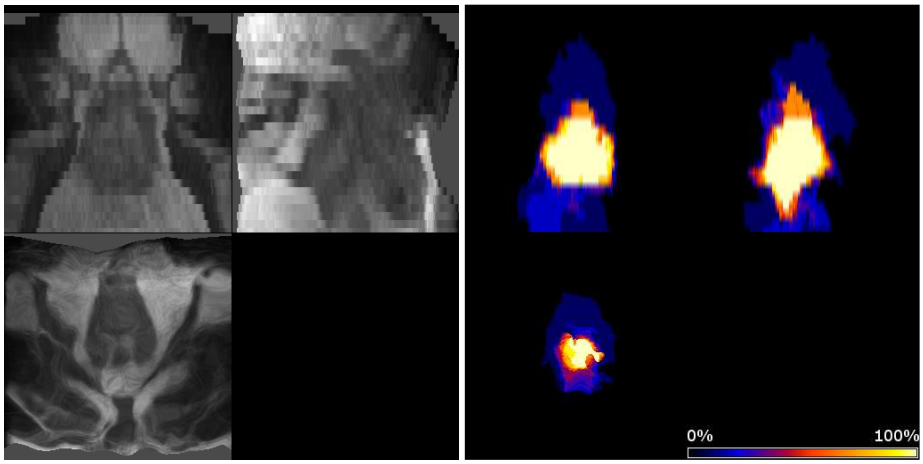


(a) (b)

**Figure 4** (a) Shows the average shape atlas from Figure 2 after affine and non-rigid registration to the test volume (shown in Figure 3). The automatic segmentations from registration of the probabilistic atlas to this volume are shown on the right (b).

Figure 7 presents a box and whisker chart describing the effects of different thresholding levels on the propagated probabilistic atlas segmentations. The low whiskers are reflective of the three cases which failed to register. A threshold of 50% is commonly used in the literature and appears to be suitable for the set of scans in this study.

(a)

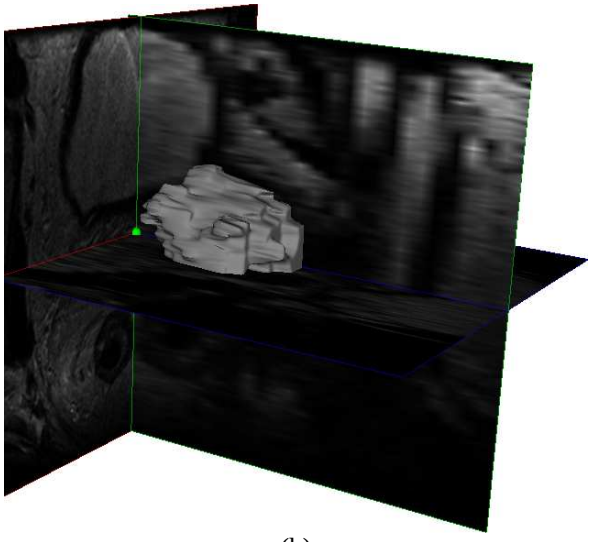

(b)

**Figure 5**. (a) Displays an axial slice from the test volume with the automatic prostate segmentation overlaid. On the right (b), a mesh has generated from the automatic prostate segmentation and is shown overlaid on the test volume.

## 4. Discussion and Conclusion

The automatic segmentation of the prostate from axial MR images using a probability atlas scheme had good correspondence with the manual segmentation

results, and may provide useful initial constraints for further segmentation methods (for example, by masking the an image and then using active contours within the masked region).

These results were constrained by the small number of MR scans (n=15) reducing the amount of variation in organ shape, and a greater number of cases should improve results. Although not used in this paper, the use of image preprocessing (particularly bias field correction), edge localization and 3D statistical shape model fitting should allow more accurate and robust localised segmentation of the organs of interest. In addition a dynamic multi-atlas selection scheme (where only the most similar scans are used to generate custom atlases), such as the one employed by Klein et al. [2] should also result in slightly higher DSC scores.

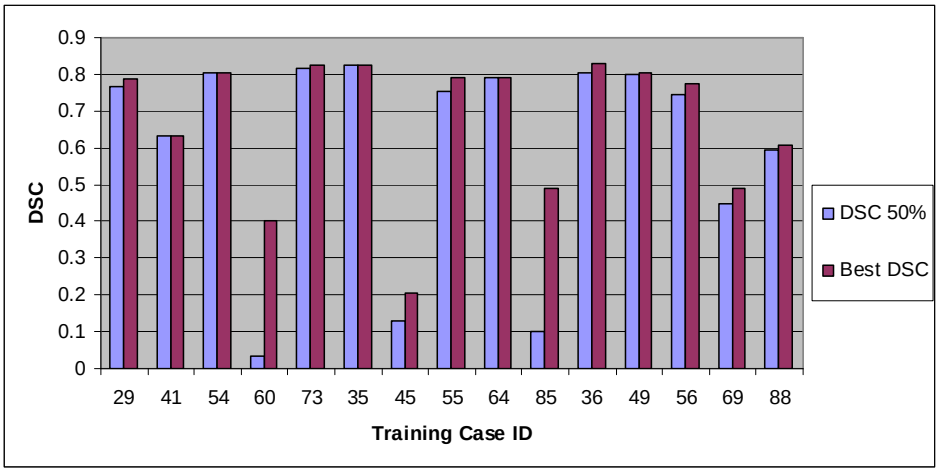


**Figure 6.** DSC scores between manual and automatic segmentations of the prostate for each training volume. Two results are provided for each case: the DSC when the prostate probabilistic atlas was thresholded at 50%, and also best DSC result for that scan over all threshold levels. Note that in this experiment the average atlas did not register correctly to volumes 60, 45 and 85 due to significant bias field artefacts (pre-processing should drastically increase the overlap for these volumes).

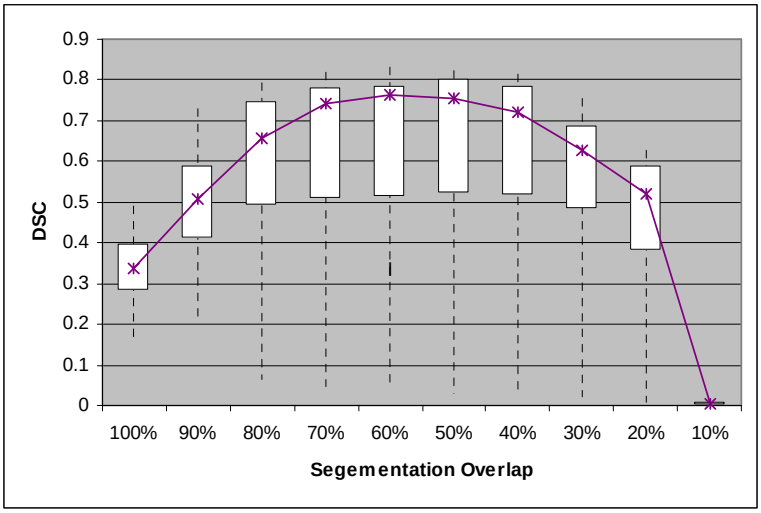


**Figure 7.** Box and whisker chart showing the segmentation overlap between manual and automatic prostate segmentation at different threshold levels (from 100% to only 10%) of agreement in probabilistic segmentation. The box shows the first quartile, the median (asterisk) and the the third quartile of the data. The whiskers display the total range of the data. The lower results are from cases 60, 45 and 85 and should be improved through bias field correction on these scans.

**Acknowledgments.** This work was partially funded by the Cancer Council NSW, Project Grant RG 07-06.

## References

1. Martin, S., V. Daanen, and J. Troccaz, *Atlas-based prostate segmentation using an hybrid registration.* Int J CARS, 2008. **3**: p. 485-492.
2. Klein, S., et al., *Automatic segmentation of the prostate in 3D MR images by atlas matching using localized mutual information.* Med Phys, 2008. **35**(4): p. 1407-17.
3. Crum, W.R., T. Hartkens, and D.L. Hill, *Non-rigid image registration: theory and practice.* Br J Radiol, 2004. **77 Spec No 2**: p. S140-53.
4. Rohlfing, T., et al., *Evaluation of atlas selection strategies for atlas-based image segmentation with application to confocal microscopy images of bee brains.* Neuroimage, 2004. **21**(4): p. 1428-42.
5. Rueckert, D., et al., *Nonrigid registration using free-form deformations: Application to breast MR images.* IEEE Trans Med Imaging, 1999. **18**(8): p. 712-21.
6. Mattes, D., et al., *PET-CT image registration in the chest using free-form deformations.* IEEE Trans Med Imaging, 2003. **22**(1): p. 120-8.
7. Dice, L.R., *Measures of the Amount of Ecologic Association Between Species.* Ecology, 1945. **26**(3): p. 297-302.